Design of a Heat Treatment for Sandvik 13C26 Maraging Steel Utilizing the Genetic Algorithm Approach to Materials Design

Joseph Ong, Monika Rolinska & Boyu Xue

2020-06-17
MH2048 Advanced Materials Design
KTH Royal Institute of Technology, Stockholm, Sweden

Abstract

This work utilizes an Integrated Computational Materials Engineering approach combined with a genetic algorithm to improve the heat treatment of the existing commercial steel alloy Sandvik 13C26. The alloy is used for knives and razor blades, and the main features are precipitates of M_7C_3 and $M_{23}C_6$ in a martensitic matrix. The optimization of the heat treatment is performed in an integrated scheme including thermodynamic tools coupled with a genetic algorithm, by maximizing a fitness function that takes into consideration the strengthening contribution of precipitate phases, with a minimum martensite fraction as a condition.

The optimal heat treatment was found to be cooling from the austenitization temperature (1250°C) to 938°C, soaking for 15 seconds, quenching, heating to 627°C, and tempering for 19 seconds.

Keywords:
Stainless steels; Thermodynamics; Precipitation; Alloy design; Martensitic formation, Genetic algorithm.

1. Introduction

Knife steels are characterized by a fine microstructure and high hardness, where the strengthening contribution comes mainly from precipitates and the fraction of martensite formed. In this work, the Sandvik 13C26 alloy is optimized regarding strength with the help of a genetic algorithm approach to materials design.

1.1 The Sandvik 13C26 Alloy

Sandvik 13C26 is a martensitic stainless steel mainly used for razor blades, surgical knives and in industrial applications for food processing. The material has a high hardness (55-62 HRC) combined with good corrosion resistance and very good wear resistance. The composition is specified in Table 1 [1].

Table 1- Chemical composition of the alloy in mass percent.

C	Si	Mn	P	S	Cr	Fe
0.68	0.4	0.7	≤0.025	≤0.010	13.0	balance

After rolling, the alloy is heat-treated in several steps to form M_7C_3 and $M_{23}C_6$ carbides as well as martensite. The heat treatment involves austenitization, cooling to a soaking temperature, soaking, quenching, and tempering, schematically shown in Figure 1. During the soaking, M_7C_3 precipitates are formed in an austenitic matrix. After quenching, we obtain a martensitic matrix, and during the tempering both M_7C_3 and $M_{23}C_6$ precipitates are formed, according to the step diagram in Figure 2.

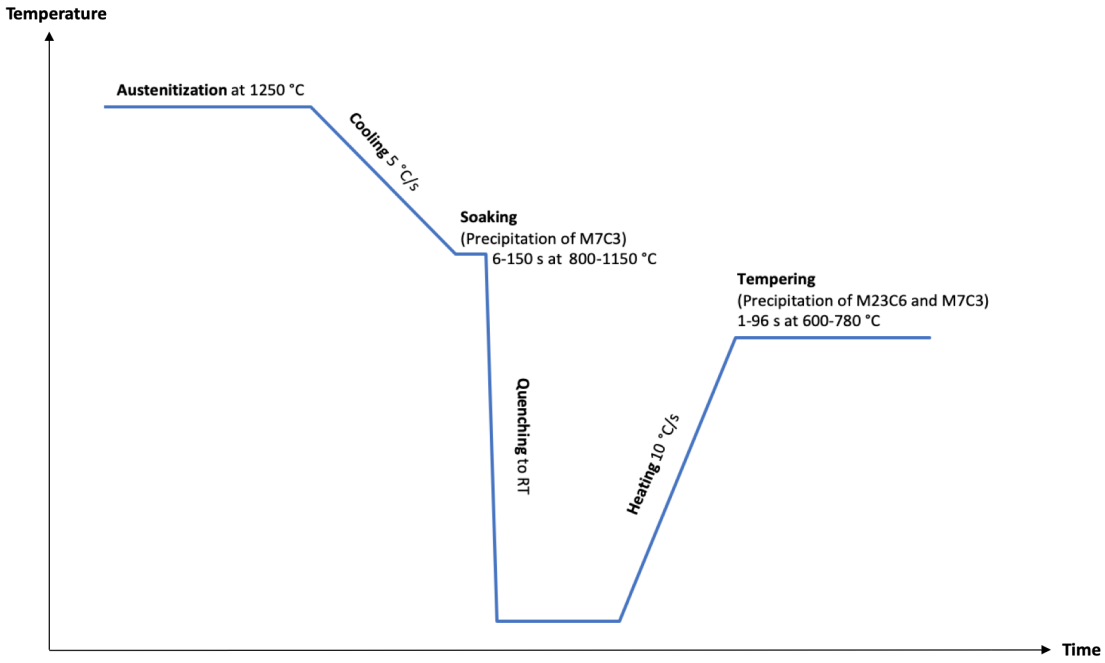

Figure 1- The heat treatment temperature profile.

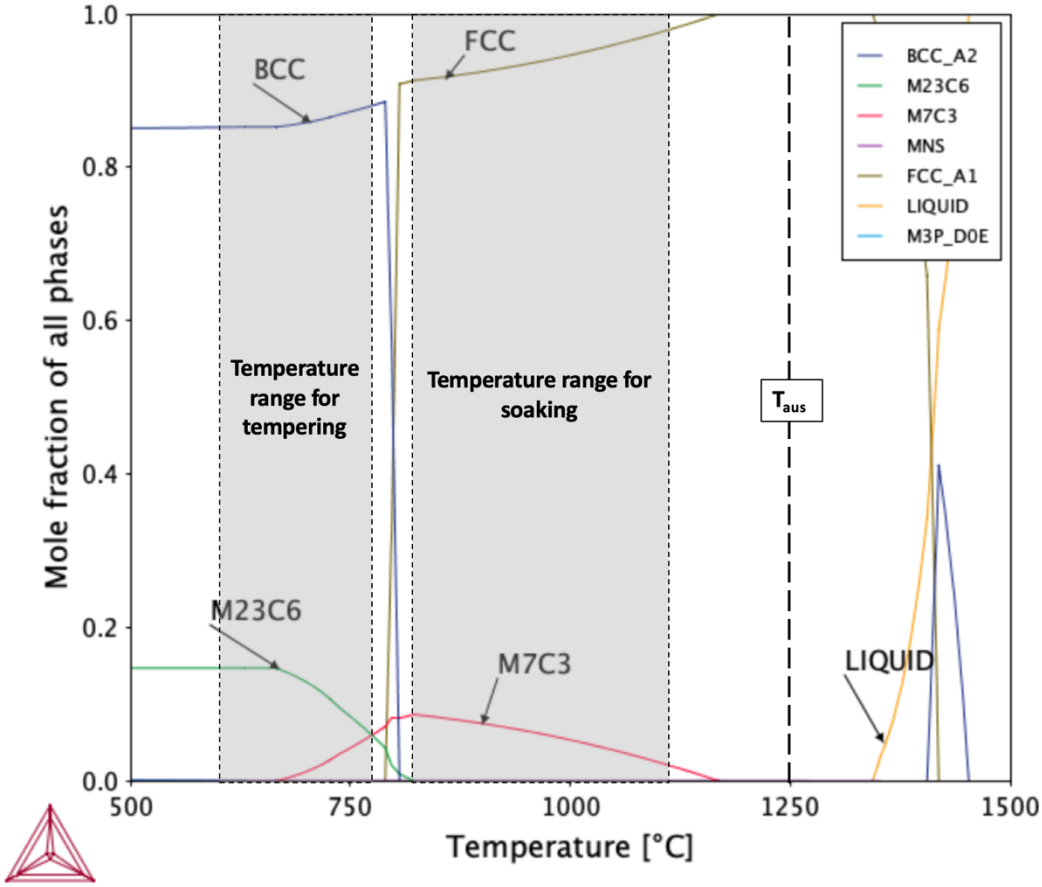

Figure 2- Step diagram of Sandvik 13C26 showing the equilibrium fractions at different temperatures and the suggested temperature ranges for the heat treatment.

The martensitic matrix is significantly strengthened by the precipitates obtained during the heat treatment. The strengthening contribution $\Delta\sigma_p$ is a mix of two strengthening mechanisms, $f^{-1/2}r^{1/2}$ is the mixed shear mechanism and $f^{-1/2}\ r^{-1}$ is the by-pass mechanism. Thus $\Delta\sigma_p$ is proportional to $f^{1/2}\ r^{-1/2}$ where f is the precipitate volume fraction and r is the mean particle radius [2] where one can soon realize that a high number density of particles is optimal for high strength.

The systems design chart in Figure 3 shows the most important features for this work for how the processing is linked to the structure and properties. This research is focused on the heat treatment processes which are related to the martensitic matrix and carbides precipitate. In this work, only the heat treatment steps after rolling are considered and thus only this part is linked to the structure. However, also the initial processing steps will have an impact on the final properties, which could be used in a more elaborate model.

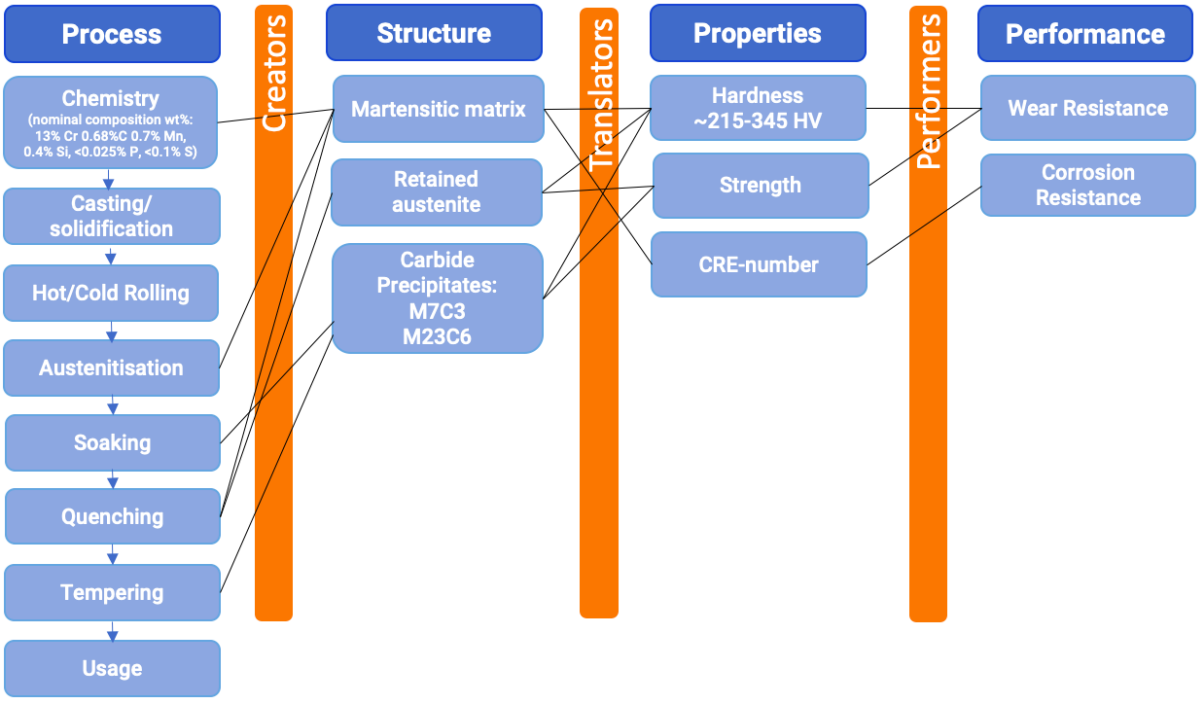

Figure 3- Systems design chart for Sandvik 13C26 including the most relevant features for the scope of this report.

1.2 The Genetic Algorithm Approach to Materials Design

There are different approaches to materials design. The common goal is to optimize material properties for a given performance. The genetic algorithm (GA) approach which is inspired by evolution theory can be used in order to optimize the properties. In all cases of materials design linkage tools are needed to show the relationship between process, structure, and properties. In the genetic algorithm approach, the linkage tools are then integrated with an optimization scheme, the genetic algorithm. The algorithm then tests different generated data sets in order to maximise the value of a so-called fitness function, that is chosen by the user.

Generally, the GA can be used for optimisation of any problem. The algorithm tries to maximise the value of the fitness function by testing different combinations [3]. In this case, we want to optimise mechanical properties of a material. The user specifies ranges to be tested for the algorithm (for example compositions, temperatures or times), and the GA starts with randomly generating a first population. A population is a set of individuals, where each individual is a combination of parameters. The parameter sets that are generated are then used in the coupled programs, and the values obtained are used as input for the fitness function. The algorithm then generates a new population by using new randomly chosen parameter sets as well as the individuals that performed well in the previous simulation as parents. Each new iteration is called a generation.

The parameter sets are presented as binary strings in the code, and each binary string is called a chromosome. In the same way as in biology, the chromosomes of the parents combine, generating new individuals with mixed properties. The code can also be modified in a way so that more or fewer mutations (changes in the chromosome) occur, giving individuals new properties. The mutations in a genetic algorithm are simply “bit flips”, where the value in the string can change from 0 to 1 if a mutation occurs [4]. This can lead to performing calculations on unexpected combinations that could easily be omitted by a human [5]. A selection of the parameters that can be modified is summarized in Table 2.

Table 2- Summary of parameters that can be changed in the GA [6].

Input variable name	Explanation
icreep	This parameter can enable (icreep=1) or disable (icreep=0) the occurrence of creep mutations. Creep mutations are added to the code for "real-life representation" and are mutations where random genes are selected, and their value changed in a range somewhere within the bounds set in the code [7].
ielite	This parameter is used to enable (ielite=1) or disable (ielite=0) elitism. Elitism means that only parents with high fitness values will be able to produce offspring.
maxgen	Sets the maximum number of generations to run by the GA.
nparam	Sets the number of parameters in an individual.
npopsize	Sets the population size.
nposibl	An array of possibilities per parameter, typically 2^n.
pcreep	The probability of creep mutation, will range between 0 and 1.
pcross	The probability of crossover. Crossover is the combination of information from a parent to form an offspring (also called recombination). The value will range between 0 and 1.
pmutate	The probability of jump mutation. A jump mutation is a "bit-flip" in a randomly selected bit. The value will range between 0 and 1 [4].

Once the algorithm is set up and the framework is established, new iterations occur until the desired number of generations is reached. A large amount of generations with many individuals in each population allows for testing of very large data sets, but with increasing size of populations comes an increasing demand for computational power. This approach thus has both advantages such as the possibility to test a lot of different combinations and the minimized bias of the human, but also some disadvantages as the required computational power and time needed for solving complex problems [2]. The settings recommended by David L. Carroll et al., the creators of the GA used in this work, are [6]:

i. npopsiz=100, pcross=0.5, pmutate=0.01, pcreep=0.02, maxgen=26
ii. npopsiz= 50, pcross=0.5, pmutate=0.02, pcreep=0.04, maxgen=51.

1.3 Purpose

The purpose of this work is to design the heat treatment (temperature and time) of the Sandvik 13C26 alloy, with the aim of maximizing the strength. The fitness function takes into account the volume fraction and mean size of precipitates, with the martensite volume fraction a condition.

2. Method

In order to optimize the heat treatment, various linkage tools have to be incorporated into the optimization scheme. Thermo-Calc and TC-Prisma are used as creator tools to relate the time and temperature to the structure, and an equation relating the mean size and volume fraction of the precipitates to the strength is used as a translator tool. In order to set up the optimization scheme, initial simulations were performed in Thermo-Calc, TC-Prisma and in TC-Python. The TC-Python code was then coupled with the GA. Finally, some adjustments were made to the GA-code parameters in an attempt to make the code more efficient.

2.1 Initial Simulations

2.1.1 Thermo-Calc and TC-Prisma

The simulations always start from a fully austenitic structure, therefore the austenitization temperature had to be found. The austenitization temperature was chosen inside the one-phase region in which only austenite is present (Fig. 2). Then the suitable range for precipitation of M_7C_3 was determined by choosing a region where only austenite and M_7C_3 were present. This was followed by non-isothermal precipitation calculations, in order to confirm the range. The temperature range for tempering was chosen in a similar way, but here the three-phase region with ferrite, M_7C_3 and $M_{23}C_6$ was chosen in order to avoid the region where austenite is in equilibrium with ferrite (which would lead to equilibrium fractions of austenite after quenching, decreasing the final amount of martensite formed).

Initial precipitation calculations were also performed to find ranges for the holding time for soaking and tempering. The assumption was that the optimal strengthening contribution will be close to the holding time where we have maximal number density of the precipitates. Therefore, isothermal precipitation calculations for the maximum and minimum temperature were performed, and the time at which we had a maximum number density for both temperatures were used as the time range. For tempering, the matrix composition will no longer be the nominal one due to the depletion of certain elements in the matrix due to carbide formation. Therefore, to obtain a guess for the holding time for the second precipitation during tempering, first non-isothermal precipitation simulations of M_7C_3 during soaking were performed. After that, the matrix composition was recorded and then isothermal simulations of M_7C_3 and $M_{23}C_6$ precipitation during tempering were performed with the obtained matrix compositions.

2.1.2 Initial TC-Python Simulations

In order to make sure that the code was set up in a correct manner, initial simulations of the entire heat treatment (with arbitrarily chosen values for temperature and time) were performed. The TC-Python code couples TC-Prisma used for precipitation calculations together with the martensite property model in Thermo-Calc.

The heat treatment profile is schematically presented in Figure 1. 1250°C was chosen as the austenitization temperature, and cooling at a rate of 5°C/s [8] was simulated down to the soaking temperature of 800°C. Soaking was simulated for 15 seconds, followed by simulation of quenching to room temperature. Prior to quenching, the matrix composition after precipitation of M_7C_3 and size distribution of the precipitates was recorded, in order to be used in the following heat-treatment steps. After that, heating at a rate of 10°C/s to the tempering temperature of 670°C was simulated, followed by simulation of tempering for 60 seconds. The tempering started from the previously recorded size distribution of M_7C_3 and during the tempering, both M_7C_3 and $M_{23}C_6$ precipitated.

2.2 Genetic Algorithm

The genetic algorithm optimization scheme was coupled with TC-Python to perform precipitation calculations (using TC-Prisma) as well as martensitic volume fraction calculations (using the martensite volume fraction property model in Thermo-Calc). The output with the mean size and volume fraction of precipitates was used in the fitness function (Equation 1). The martensite volume fraction was used as a condition to obtain a strengthening effect, in order for the fitness function to incorporate the obtained results, the martensite volume fraction had to exceed 0.75, as Safara et al. suggested that optimal mechanical properties were achieved around a martensitic fraction of 0.85 [8]. This condition was set as an alternative to a go/no go-criterion, which is discussed further in Section 3.

The fitness function for strength optimization with regard to precipitation is based on Equation 1 [9] where *f* is the volume fraction of precipitates, *r* is the mean size of precipitates, *G* is the shear modulus and *b* is the Burger's vector in the lattice.

$$\Delta\sigma_p = 1.66\, G\, b \frac{\sqrt{f}}{r} \qquad \text{Equation 1}$$

The volume fraction and mean size of precipitates are obtained from TC-Prisma simulations. The shear modulus is calculated by Equation 2 [10], and Burger's vector with equation 3 using values specified in Table 3 [10].

$$G = G_0 \left[1 + G_1 \frac{T[K] - 300}{T_m[K]}\right] \qquad \text{Equation 2}$$

$$b = b_0[1 + b_1 T[°C]]$$ Equation 3

Table 3 -Input values for obtaining of the shear modulus and Burger's vector.

Parameter		Parameter	
T[K]	298	T_m[K]	1810
G_0 [MPa]	6.40E+04	G_1 [-]	-8.10E-01
B_0 [m]	2.48E-10	B_1 [-]	-

The nominal composition specified in Table 1 was used as an input for all the simulations. The temperature range and time range were found with the initial simulations in Thermo-Calc and TC-Prisma mentioned in Section 2.1.1. The other variables for the GA are presented in Table 4. A summarizing flowchart is presented in Figure 4.

Table 4, Input variables used in the GA

npopsiz	**pcross**	**pmutate**	**pcreep**	**maxgen**	**nposibl**
5	0.5	0.02	0.04	51	64

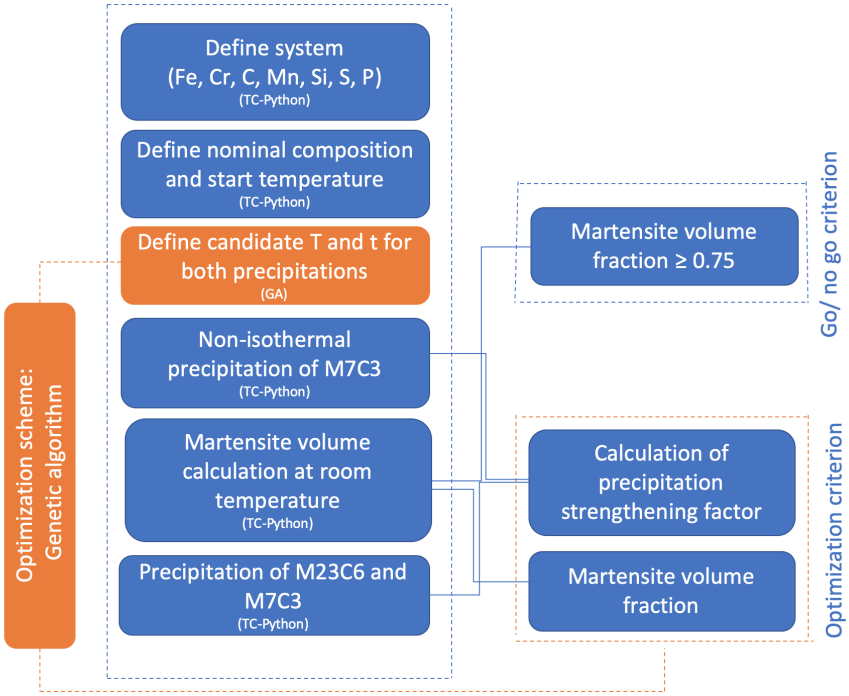

Figure 4- Summarizing flowchart of the GA

2.3 Improvement of the Optimisation Scheme

The main objective of the improvement of the Genetic Algorithm optimization process would be to maximize the fitness function in the shortest possible time frame with reasonable results. For the Genetic Algorithm we seek to tinker various types of inputs such as npop, nparam, pcreep, pcreep, pmutate, pcrossover to obtain a stable fitness function curve. In this work, the population size was varied.

3. Results and Discussion

3.1 Initial Precipitation Calculations

The austenitization temperature was chosen to be 1250°C, and the suitable temperature range for the M_7C_3 precipitation during soaking is about 800-1100°C based on the equilibrium lines shown in Figure 2. Further non-isothermal precipitation calculations proved the range to be 800-1050°C, as there were no results for higher temperatures. The difference between the results from the equilibrium calculation and the non-isothermal calculation is explained by the very high nucleation barrier at the higher temperatures. Because the non-isothermal calculation is the one used in the GA, the temperature range between 800-1050°C was chosen to be incorporated into the GA according to Fig. 2. For the tempering, the temperature range was chosen to be between 600-780°C to avoid the phase transformation from martensite (BCC) to austenite, according to Fig. 2.

The holding time range for soaking was chosen to be between 6 and 150 seconds, based on the number density peaks shown in Figure 5. In a similar way, the holding time for tempering was chosen to be between 1 and 96 seconds. These simulation results are based on the matrix composition obtained after soaking, without incorporating the size distribution of M_7C_3 formed. Including the particle size distribution would give more accurate results as it would be closer to reality, but just using the matrix composition was simply faster due to the limited knowledge of the software at the time.

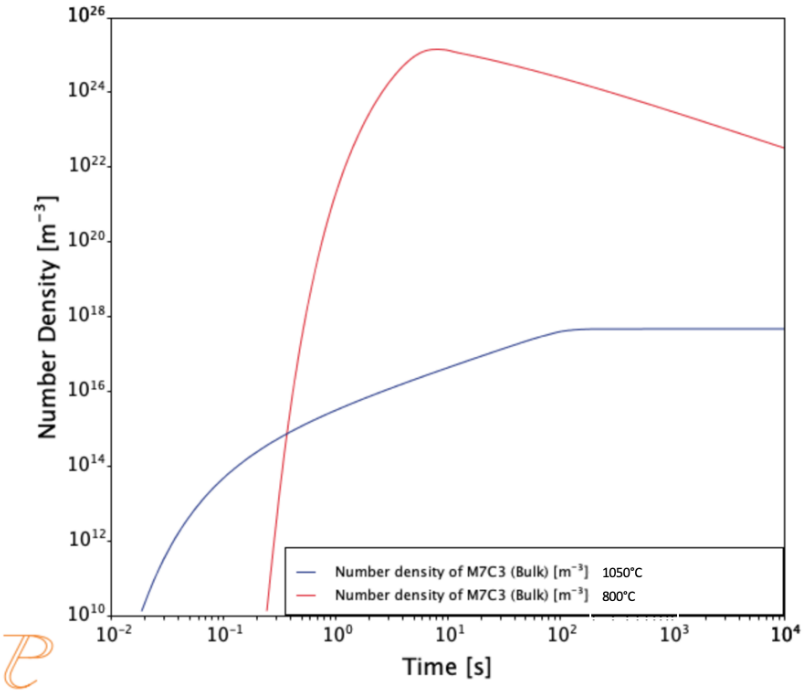

Figure 5- Number density peaks used to determine the time range for soaking.

3.2 Initial TC-Python Simulation

The precipitation of M7C3 from an austenitic matrix after cooling and soaking in 800°C was calculated by TC-Python and the results are presented in Table 5. These results were also validated in the graphical mode of TC-Prisma. The mean size, number density, volume fraction, and composition of M_7C_3, were further used as input parameters for the tempering simulation. The composition of the depleted FCC-matrix after precipitation of M_7C_3 was used as an input parameter for the martensite transformation simulation. After quenching to room temperature (300K), the martensite volume fraction was 99.301% of the matrix volume.

Table 5- Values obtained after cooling to 800°C and soaking for 15 s.

Precipitate phases	**Mean Size [m]**	**Number density [m^{-3}]**	**Volume Fraction**	**Composition of M_7C_3 [mole fraction]**	**Composition of FCC [mole fraction]**
M_7C_3	1.814e-08	2.148e+21	0.0537	Fe=0.157257418 C=0.300000000 Si=1.00213e-09 Mn=0.00312605 Cr=0.539616524 S=0.0 P=0.0	Fe=0.866116766 C=0.0119219238 Si=0.008184789 Mn=0.00710774 Cr=0.106605411 S=4.480563e-05 P=1.85541e-05

The volume fraction variation of M_7C_3 with the soaking time are shown in Fig. 6. The number density variation of M_7C_3 with the soaking time are shown in Fig.7.

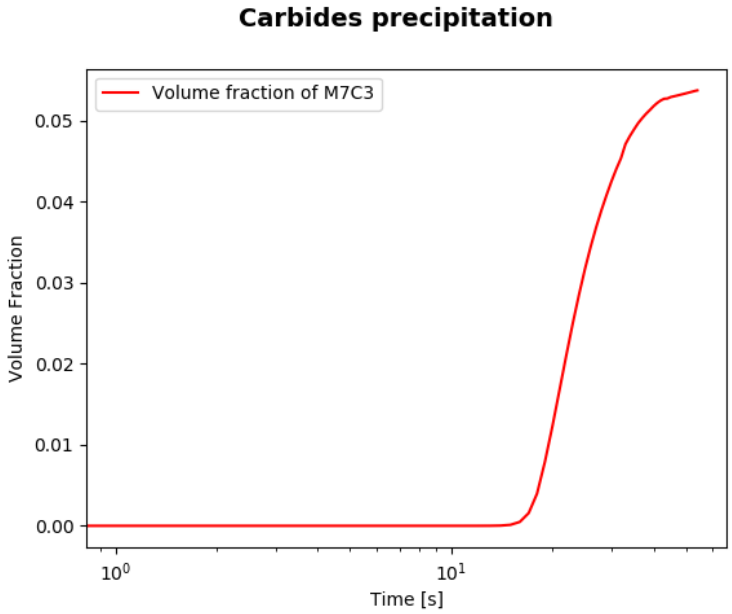

Figure 6- The change of volume fraction of M_7C_3 during 15 s of soaking at 800°C.

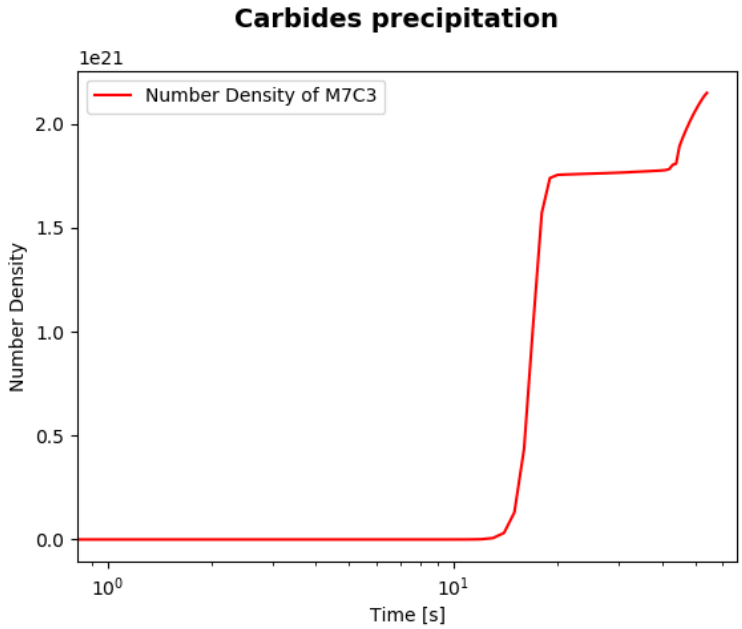

Figure 7- The change of number density of M_7C_3 during 15 s of soaking at 800°C.

The number density distribution of M_7C_3 after soaking, that is used as an input for the following tempering, is shown in Figure 8.

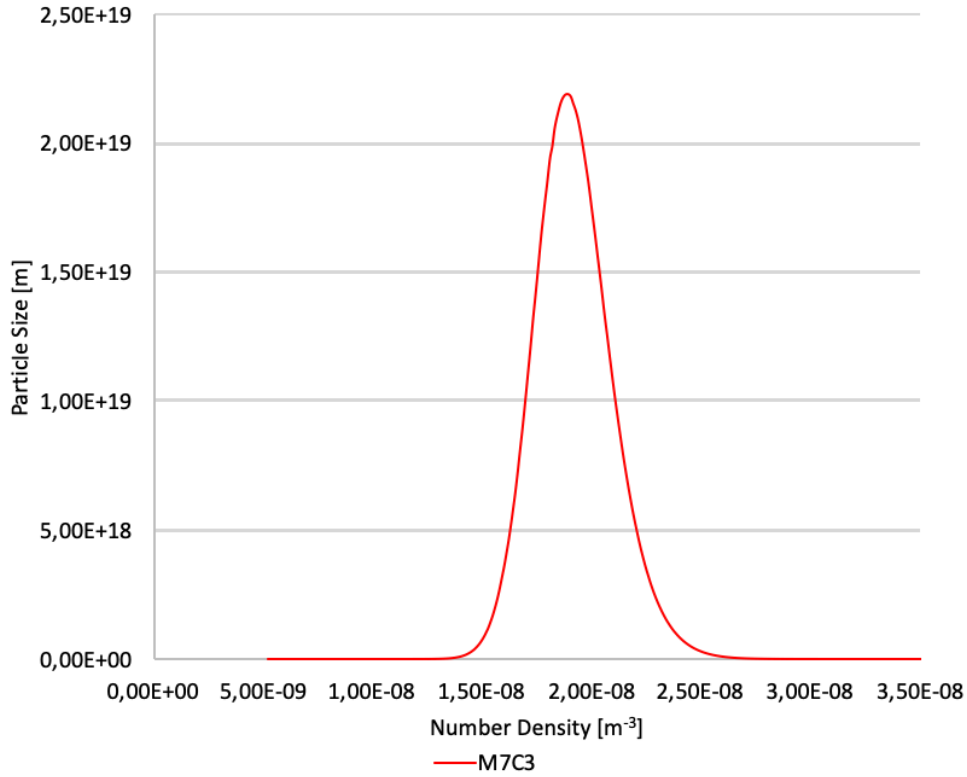

Figure 8- Number density distribution after soaking for 15 s in 800°C.

The values obtained after tempering are presented in Table 6.

Table 6- Precipitate phases after tempering at 670°C for 60s

Precipitate phases	**Mean Size [m]**	**Number density [m^{-3}]**	**Volume fraction**
M_7C_3	1.239e-08	1.038e+22	0.082652
$M_{23}C_6$	4.215e-09	5.944e+20	0.000186

The volume fraction changes of M_7C_3 and $M_{23}C_6$ during the tempering time are shown in Figure 9.

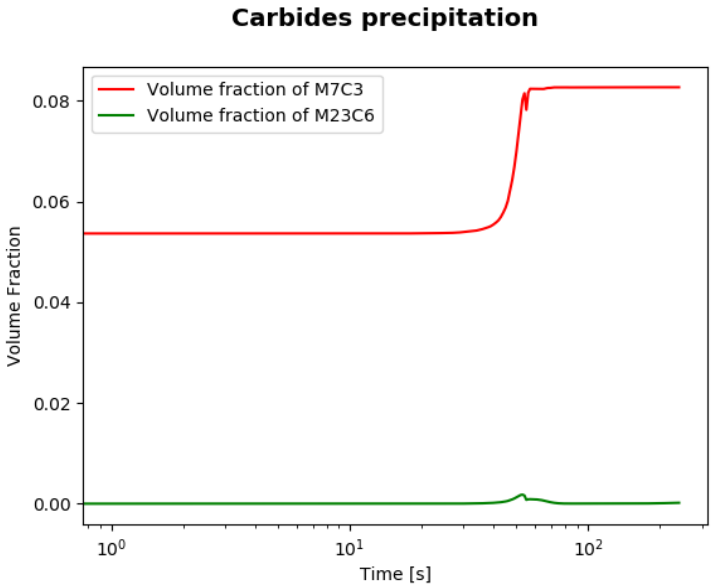

Figure 9- Volume fraction changes of $M_{23}C_6$ and M_7C_3 along the tempering time.

The number density changes of $M_{23}C_6$ and M_7C_3 along the tempering time are shown in Figure 10.

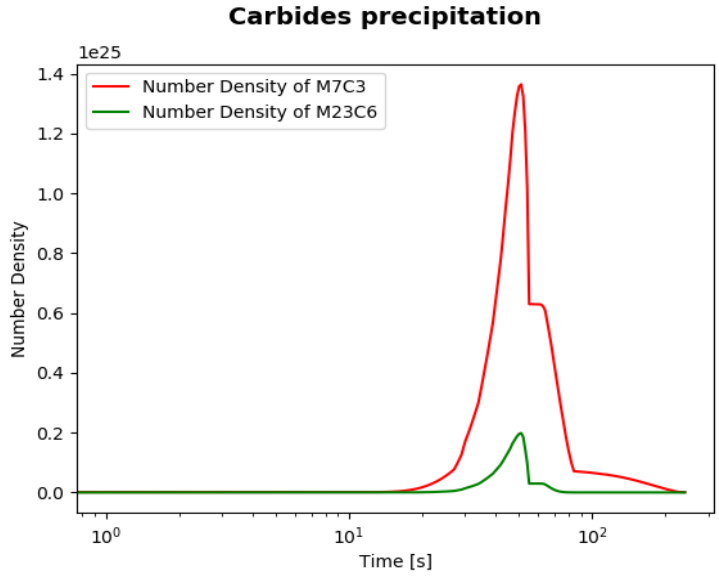

Figure 10- The number density changes of $M_{23}C_6$ and M_7C_3 along the tempering time.

Comparing Table 5 and 6 we can see that the volume fraction of M_7C_3 increases even though it should decrease according to Fig. 2. This can be explained because M_7C_3 is already present and the continued growth of the metastable phase is more favourable as the surface energy of the particles will continue to decrease. This growth of M_7C_3 is also something that has been observed experimentally before for this steel grade [11]. For longer tempering times, the stable state should be established in the material and the volume fraction of M_7C_3 should decrease as M_7C_3 will dissolve. In order to verify this assumption, a simulation of the tempering with a longer holding time (500 s) was established and the result (Fig. 11) shows that the volume fraction of M_7C_3 phase decreases drastically after 200 s of holding time.

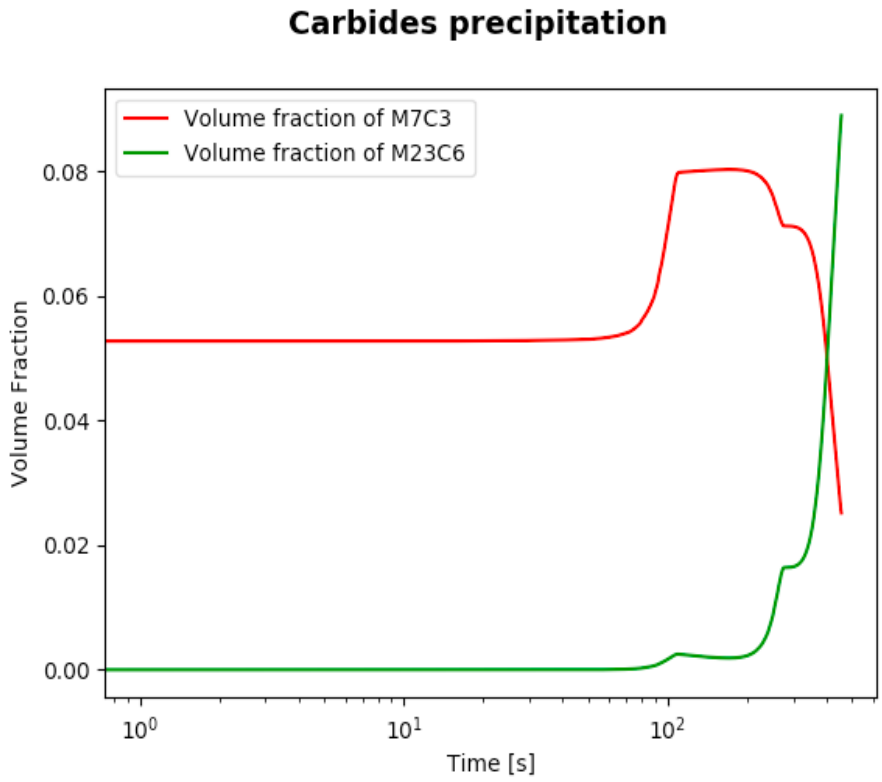

Figure 11. Volume fraction changes of $M_{23}C_6$ and M_7C_3 along tempering for 500 s.

3.3 Genetic Algorithm Simulation

Figure 12 shows how the fitness function value varies with different parameters. A selection of parameters and corresponding fitness function values is presented in Table 7.

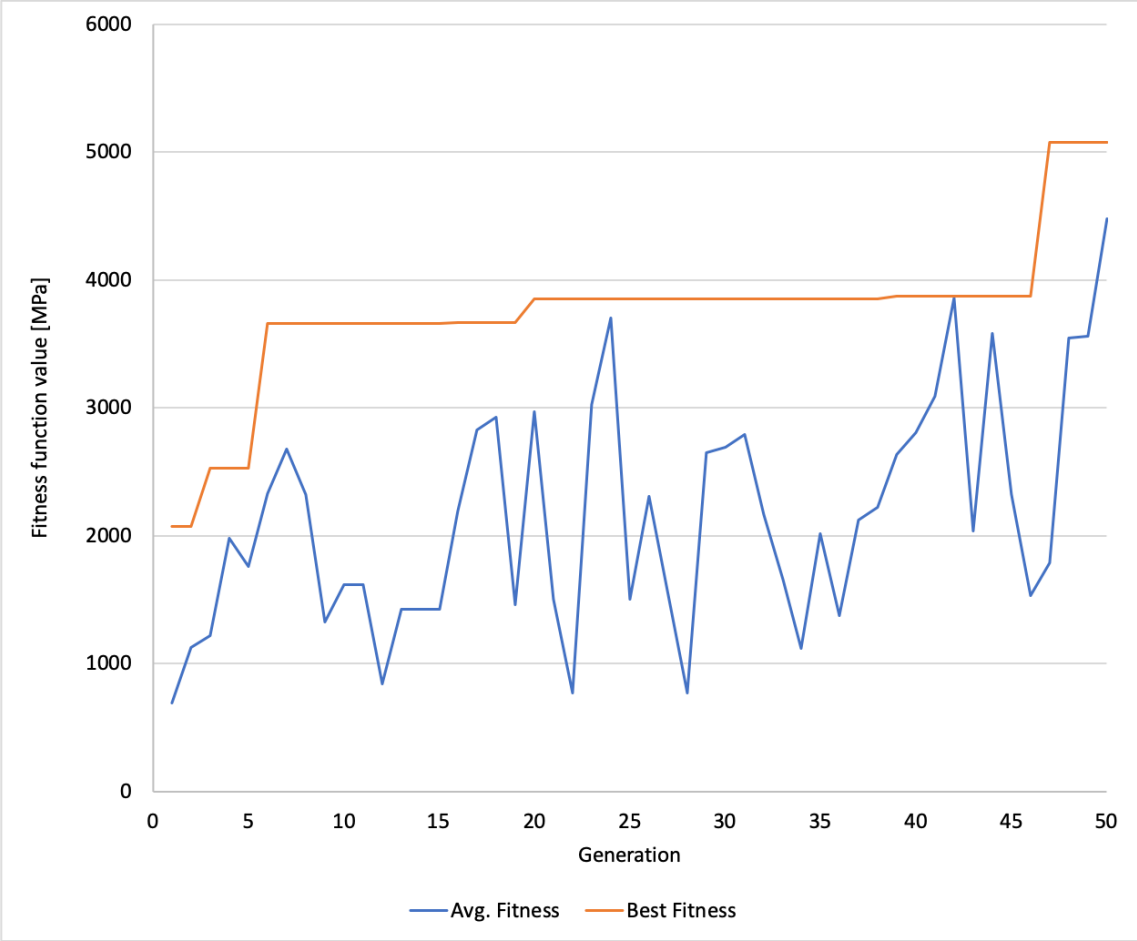

Figure-12 Fitness function value for our simulations

Table 7- Selection of variables and corresponding fitness function values

Case #	Soaking temperature [°C]	Soaking time [s]	Tempering temperature [°C]	Tempering time [s]	Fitness function value [MPa]
1	938	15	627	19	5074
2	938	15	635	19	4605
3	975	33	627	63	3665
4	975	70	627	63	3661
5	1022	111	750	27	1381
6	975	70	706	63	559
7	860	70	690	61	491
8	959	143	627	61	-*

*Martensite volume fraction <0.75

As seen in Table 7, we have a complex interplay of different parameters. Comparing case 1 and 2, a lower tempering temperature seems favourable. Comparing case 3 and 4, a shorter soaking seems favourable. However, we also see that we are not at the end-values of the specified ranges, which highlights that the relationship is not so simple. Of course, lower temperatures lead to more nucleation, and shorter times to less growth, meaning that we will have a smaller mean size. However, with too short times, the volume fraction will also stay low as the precipitates do not have time to grow at all. Lower soaking temperatures lead to longer cooling times, which will also affect the precipitation, giving a more complex distribution of particles, that is maybe not so intuitive.

The values of strength increase of over 5000 MPa are not plausible in real life. This value could be due to the limitations in our model, where the thickness of the plate, temperature gradient etc. are not considered, but this could also be due to the limitations in our code. In the fitness function we use the mean size, as the mean size does not show the real distribution. During tempering, we introduce very small precipitates, and M_7C_3 will also start to dissolve at low temperatures, decreasing the mean size. The extent to which the mean size is affected has not been investigated but changing the fitness function to include the contribution in two terms (using the mean size of M_7C_3 and $M_{23}C_6$ separately) could maybe give a fairer picture. Also using a better linkage tool that takes into consideration not only the mean size but also the particle size distribution could improve the reliability of the results. Also incorporating an equation with both the mixed-shear and by-pass strengthening mechanism could give another result for the fitness function with the same values, which really highlights how important linkage tools are. Since the tempering was not verified in Graphical mode due to technical issues, this should also be done to exclude other problems. However, the results from the single TC-Python simulation do not give any reason to believe there is a problem in the code, as Figure 9 shows that the tempering simulation does indeed start from the previous particle size distribution.

3.4 Improvement of the Optimisation Scheme

This process involves finding the best set of fitness function values in the smallest possible time. Over each iteration of the GA, we expect the shapes of the fitness function to be roughly similar with a different input parameter. Sharp dips and increments were observed over time while fitness function would come to a plateau at a later point of the iteration. These results are expected to get more and more constant along with time. This would allow companies to obtain their results efficiently and implement changes in a shorter time frame to save on opportunity costs. Final parameters that have been utilized in input file were specified in Table 4.

Npopsiz was changed from 100 (recommended by Carroll et al. [6]) to 5, as a large population size would take a significant amount of time which may not be necessary for results to be generated at a greater efficiency. Other parameters were kept according to the recommendation.

By changing the population size from 100 to 5 the simulation run time decreased by 66%, from 72 to approximately 24 hours for a stable fitness function curve that plateaus at a specific value.

To improve the efficiency of the simulation, also the ability to read the previous results should be built into the TC-Python script, which would prevent the code from simulating the cooling for all individuals (as it then should be able to start from the already existing values). A proper go/ no-go criterion where the simulation stops at an insufficient martensite volume fraction could also be incorporated to decrease the simulation time (as now the fitness function value was set to 0, but the simulation still continued).

3.5 Future Work

One important part of research is experimental validation. Validation of these results could be done in a Gleeble simulator [11], that can perform experiments on very small material amounts. The integrated scheme could be improved in various ways. In the precipitation code, default values for nucleation sites and grain sizes were used. Incorporating more complex models such as grain boundary precipitation with a more specific grain size would be interesting to look at. Since the material is rolled before the heat treatment, the dislocation density could also be incorporated. Also, consideration of the grain growth during the treatment could be the next step to integrate into the model as grain-boundary strengthening also is an important strengthening mechanism. Further development of the model for industrial purposes should also include time-ranges that are feasible in real life. Heat transfer and the temperature profile in the material could also be incorporated to make a model that is even closer to reality. To form an even more complex model, the microstructural evolution during the rolling could also be considered, as for instance, hot/cold rolling can break down the casting microstructures like dendrites and create anisotropic crystal structure.

4. Conclusion

The goal was to optimize a heat treatment of the Sandvik 13C26 maraging steel, with regards to the precipitation strengthening contribution. By maximizing the fitness function value based on mean size and volume fraction of precipitates, and excluding heat treatments resulting in a too low martensite fraction, the optimal heat treatment was: cooling from the austenitization temperature (1250°C) to 938°C, soaking for 15 seconds, quenching, heating to 627°C and tempering for 19 seconds.

5. Acknowledgment

We would like to express our gratitude to Manon Bonvalet at the Unit of Structures at the Department of Materials Science and Engineering at KTH, Stockholm for guidance and valuable discussions as well as technical help during the entire project.

References

[1] Sandvik AB, ”Sandvik 13C26 Strip Steel Datasheet,” 2018. [Online]. Available: https://www.materials.sandvik/en/materials-center/material-datasheets/strip-steel/sandvik-13c26/?show=pdff . [Accessed 6 May 2020].

[2] W. Xu, P. Rivera Diaz del Castillo och S. van der Zwaag, ”A combined optimization of alloy composition and aging temperature in designing new UHS precipitation hardenable stainless steels,” *Computational Materials Science,* pp. 467-473, 2009.

[3] D. Goldberg, Genetic Algorithms in Search, Optimization and Machine Learning, Addison-Wesley, 1989.

[4] X. An, ”Lecture Slides CSE4403 3.0/CSE6602E - Soft Computing, Lecture 9 Genetic Algorithms & Evolution Strategies,” 2011. [Online]. Available: https://wiki.eecs.yorku.ca/course_archive/2011-12/F/4403/_media/cse4403lec9.pdf. [Accessed 6 June 2020].

[5] M. Walbrühl, ”Lecture notes MH2048 Advanced Materials Design, Lecture: GA,” KTH, 2020.

[6] D. L. Carroll, ”Genetic algorithm (GA),” 2001. [Online]. Available: https://engineering.purdue.edu/~eigenman/ECE563/Handouts/gafort.f90.txt.

[7] N. Soni och T. Kumar, ”Study of Various Mutation Operators in Genetic Algorithms,” *(IJCSIT) International Journal of Computer Science and Information Technologies,* vol. 5, nr 3, pp. 4519-4521, 2014.

[8] N. Safara, A. Golpayegani, G. Engberg och J. Ågren, ”Study of the mean size and fraction of the second-phase particles in a 13% chromium steel at high temperature,” *Philosohical Magazine,* nr https://doi.org/10.1080/14786435.2019.1674455, 2019.

[9] M. Walbrühl, *Home Assignment II MH2048 Advanced Materials Design,* Stockholm: KTH, 2020.

[10] G. Engberg, *Unpublished work.*

[11] M. Bonvalet, Interviewee, *Private conversation.* . 8 June 2020.